Cell, Vol. 118, 781–794, September 17, 2004, Copyright ©2004 by Cell Press

JunD Reduces Tumor Angiogenesis by Protecting Cells from Oxidative Stress

Damien Gerald,[1] Edurne Berra,[2] Yves M. Frapart,[3] Denise A. Chan,[4] Amato J. Giaccia,[4] Daniel Mansuy,[3] Jacques Pouysségur,[2] Moshe Yaniv,[1] and Fatima Mechta-Grigoriou[1,*]

[1]Unit of Gene Expression and Diseases
CNRS URA 1644
Pasteur Institute
25 Rue du Docteur Roux
75724 Paris
Cedex 15

[2]Institute of Signaling
Developmental Biology and Cancer Research
CNRS-UMR 6543
Centre Antoine Laccassagne
33 Avenue de Valombrose
06189 Nice

[3]Laboratoire de Chimie Biochimie
Pharmacologique et Toxicologique
CNRS UMR 8601
Université R. Descartes
45, Rue des Saints Pères
75270 Paris
Cedex 06
France

[4]Department of Radiation Oncology
Stanford University School of Medicine
Stanford, California 94305

Summary

Reactive oxygen species (ROS) are implicated in the pathophysiology of various diseases, including cancer. In this study, we show that JunD, a member of the AP-1 family of transcription factors, reduces tumor angiogenesis by limiting Ras-mediated production of ROS. Using *junD*-deficient cells, we demonstrate that JunD regulates genes involved in antioxidant defense, H_2O_2 production, and angiogenesis. The accumulation of H_2O_2 in *junD*$^{-/-}$ cells decreases the availability of FeII and reduces the activity of HIF prolyl hydroxylases (PHDs) that target hypoxia-inducible factors-α (HIFα) for degradation. Subsequently, HIF-α proteins accumulate and enhance the transcription of *VEGF-A*, a potent proangiogenic factor. Our study uncovers the mechanism by which JunD protects cells from oxidative stress and exerts an antiangiogenic effect. Furthermore, we provide new insights into the regulation of PHD activity, allowing immediate reactive adaptation to changes in O_2 or iron levels in the cell.

Introduction

Maintaining oxygen (O_2) homeostasis is essential for survival. Change in O_2 pressure is a major stimulus that elicits rapid cellular responses. Hypoxia leads to the transcription of genes that help supply O_2 to tissues by inducing glycolysis, erythropoiesis, and angiogenesis. The transcription factor HIF (hypoxia-inducible factor) is an essential element of this cellular response (for reviews, see Semenza [1999]; Giaccia et al. [2003]; Pugh and Ratcliffe [2003a]). HIF induces the transcription of genes such as vascular endothelial growth factor (*VEGF-A*), glucose transporter 1 (*Glut1*), and erythropoietin (*Epo*). Their promoters contain at least one hypoxia response element (HRE) that is bound by HIF, heterodimer composed of one of the three α subunits (HIF-1α, HIF-2α, or HIF-3α) and the β subunit (HIF-1β or ARNT [aryl hydrocarbon nuclear translocator]) (for review, see Wenger [2002]). Although HIF-1β is constitutively expressed, HIF-α subunits are short-lived proteins. Under normoxic conditions, the HIF-1α protein interacts with the von Hippel-Lindau tumor suppressor protein (VHL) (for reviews, see Kim and Kaelin [2003]; Pugh and Ratcliffe [2003b]). VHL belongs to an E3 ubiquitin ligase complex that targets HIF-1α for degradation by the proteasome. The interaction between HIF-1α and VHL depends on hydroxylation of HIF-1α on critical proline residues (Ivan et al., 2001; Jaakkola et al., 2001). These hydroxylations are catalyzed by the HIF prolyl hydroxylases (PHDs) enzymes (Bruick and McKnight, 2001; Epstein et al., 2001). Full enzymatic activity of PHDs requires O_2, 2-oxoglutarate, and ferrous iron (FeII) for function. Under hypoxic conditions, PHD activity is decreased. HIF-1α protein thereby lacks hydroxylation and accumulates in the cells.

The hypoxic induction of angiogenesis is a hallmark of many pathologies, such as solid tumor progression. Tumor angiogenesis increases tumor growth beyond a limited size (i.e., 1–2 mm in diameter) and promotes the metastatic spread of tumor cells (for review, see Folkman [1990]). One example of such adaptive proliferative and angiogenic functions is provided by the Ras oncogene. Constitutively activated forms of Ras have been described as the most common mutated oncogene detected in human tumors (Barbacid, 1987; Bos, 1989). Constitutive Ras signaling results in loss of contact inhibition and abnormal cell proliferation (Peeper et al., 1997). Moreover, overexpression of Ras has been linked to vascularization of tumors (Bergers and Benjamin, 2003). Indeed, transformation by Ras stabilizes HIF-1α and upregulates the transcription of *VEGF-A*. Activated forms of Ras have also been correlated with the production of high amounts of reactive oxygen species (ROS) (Irani et al., 1997). Moreover, chemical antioxidants inhibit the mitogenic activity of Ras, indicating that ROS participate directly in malignant transformation. Finally, ROS stabilize HIF-1α protein and induce production of angiogenic factors by tumor cells (Chandel et al., 1998). Oxidative stress is thus assumed to play a key role in tumor angiogenesis and cancer progression.

The AP-1 transcription factor plays a central role in modulating transformation by Ras (for review, see Mechta-Grigoriou et al. [2001]). AP-1 is composed of Jun family members (c-Jun, JunB, and JunD) that can form either homo- or heterodimers among themselves or with the Fos family members (c-Fos, FosB, Fra1, Fra2). The dif-

*Correspondence: fmechta@pasteur.fr

ferent AP-1 dimers exhibit rather similar DNA binding specificities but differ in their transactivation efficiencies. Studies of AP-1 functions in cell culture and in mouse models reveal distinct roles for each member (for reviews, see Wagner [2001]; Shaulian and Karin [2002]). The three *jun* genes exhibit different expression patterns during cell cycle progression. While *c-jun* and *junB* behave as immediate early genes upon mitogenic stimulation, *junD* expression remains almost invariant, and its product is partially degraded upon serum-induced reentry into the cell cycle (Pfarr et al., 1994). Moreover, overexpression of JunD in immortalized fibroblasts slows their proliferation and induces accumulation in the G1 phase. Furthermore, immortalized fibroblasts lacking *junD* (*junD*$^{-/-}$) display higher proliferation rates than their wild-type (wt) counterparts (Weitzman et al., 2000). In contrast, c-Jun overexpression stimulates S phase entry, and c-Jun function is required for cell cycle progression (Kovary and Bravo, 1991; Wisdom et al., 1999).

The antagonistic balance in the function of the different Jun members is also illustrated by their respective roles in transformation. While c-Jun cooperates with Ras, excess JunD partially suppresses the transformed phenotype of the cells (Pfarr et al., 1994; Mechta et al., 1997). The negative effect of JunD is mainly attributed to its ability to slow fibroblast growth. Since angiogenesis is a crucial step in tumor progression, we investigated the function of JunD in this process. In this paper, we show that overexpression of JunD downregulates *VEGF-A* expression and reduces angiogenesis in tumors. Moreover, we demonstrate that JunD protects cells from oxidative stress by limiting ROS production. Microarray analysis reveals that JunD acts both on cellular antioxidant defense systems and H_2O_2 production. Taking advantage of *junD*-deficient cells, we show that accumulation of oxidants such as H_2O_2 decreases the proportion of PHD in FeII oxidation state, thereby inhibiting its enzymatic activity. This inhibition impairs the degradation of HIF-1α under normoxia and enhances *VEGF-A* transcription. This study provides new insights into the mechanism of iron-dependent regulation of PHD activity and uncovers how JunD displays an antiangiogenic effect by promoting HIF-α degradation.

Results

Overexpression of JunD Reduces Ras-Induced Tumor Angiogenesis

We have previously shown that JunD overexpression slows Ras-induced tumor growth (Pfarr et al., 1994). In this study, we used 3T3 cells transformed by the Ki-ras oncogene (Ras) and three independent clonal lines with increased JunD expression (Ras+junD). After subcutaneous injection into nude mice, we repeatedly observed that tumors derived from the different Ras+JunD cell lines were paler than those derived from Ras cells. We therefore monitored the vascular content of these tumors when they had reached the same size. Tumors derived from Ras-transformed cells were highly vascularized and hemorrhagic (n = 18 tumors) (Figures 1Aa and 1Ab). In contrast, tumors derived from the three independent Ras+JunD cell lines remained pale and poorly vascularized (n = 36 tumors) (Figures 1Ac and 1Ad). Histological analysis of sections stained with an endothelial-specific antibody (PECAM-1) confirmed these macroscopic observations (Figure 1B). The vascular density was reduced in tumors from Ras+JunD clones (Figures 1Be–1Bh and 1C) compared to Ras cells (Figures 1Ba–1Bd and 1C). Ras+JunD tumors had fewer vessels with occasional avascular areas (Figure 1Bg). Finally, the proportion of large-sized vessels was higher in Ras- than in Ras+JunD-derived tumors (Figure 1C), indicating that overexpression of JunD reduces the number and the size of the blood vessels.

JunD Controls the Rate of *VEGF-A* Transcription

Many oncogenic pathways trigger induction of the major angiogenic factor VEGF-A (for review, see Ferrara et al. [2003]). Moreover, even modest decreases in *VEGF-A* expression led to a marked reduction of tumor angiogenesis (Benjamin and Keshet, 1997). We therefore measured the level of *VEGF-A* mRNA expression by quantitative (Q) real-time RT-PCR experiments. JunD overexpression significantly decreased the level of *VEGF-A* mRNA in tumors (Figure 2A) and Ras-transformed cells (Figure 2B). Upon hypoxia, the accumulation of *VEGF-A* mRNA proceeds by both transcriptional induction and stabilization of its mRNA. To evaluate the contribution of these two processes, we measured the level of the primary transcript of *VEGF-A* by amplification of an intron (intron 4). Results shown in Figure 2B confirm that JunD reduced the rate of *VEGF-A* transcription in Ras-transformed cells.

To further assess the role of JunD in the regulation of *VEGF-A*, we measured the level of *VEGF-A* mRNA in immortalized fibroblasts derived from *junD*$^{-/-}$ embryos. Three independent wt and *junD*$^{-/-}$ cell lines were isolated and used for further experiments (see Supplemental Figure S1). Steady-state levels of *VEGF-A* mRNA were increased in *junD*$^{-/-}$ fibroblasts as compared to control cells (2.5-fold) (Figure 2C). The primary transcript of *VEGF-A* exhibited similar amplification as its mRNA in *junD*$^{-/-}$ cells, confirming that JunD-mediated effect is transcriptional. Finally, to verify that the accumulation of *VEGF-A* mRNA in *junD*$^{-/-}$ cells was not due to the immortalization protocol, we checked the level of *VEGF-A* transcripts in *junD*$^{-/-}$ embryos (10.5 dpc) by semiquantitative RT-PCR (Figure 2D). Pools of four embryos were analyzed to avoid individual variations. We repeatedly detected an upregulation of *VEGF-A* expression in *junD*$^{-/-}$ embryos. Thus, the enhanced *VEGF-A* transcription results from the deletion of *junD* and is independent of the immortalization state of the cells.

The upregulation of *VEGF-A* transcription in the *junD*$^{-/-}$ cell lines was confirmed by transient transfection assays using the human *VEGF-A* promoter (P-1176) (Figure 2E), a construct that triggers *VEGF-A* expression under hypoxic conditions (Ikeda et al., 1995). Deletion of the region (−1176 to −888) completely abolished the effect of *junD* (Figure 2E). Since the deleted region contains a potential AP-1 binding site, we tested if AP-1 may directly regulate the promoter. Cotransfection of

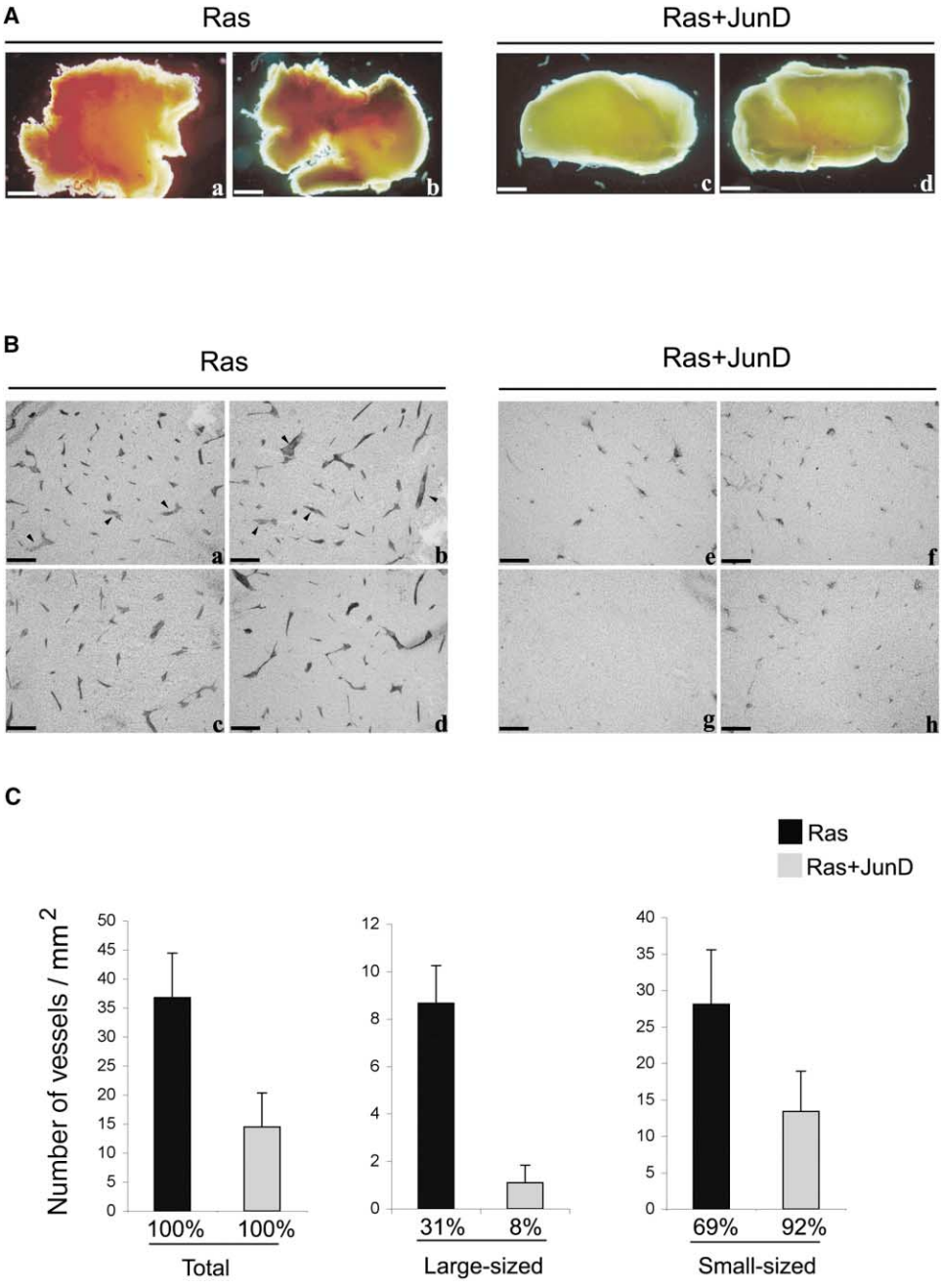

Figure 1. Overexpression of JunD Reduces Tumor Angiogenesis

(A) Representative views of tumors derived from Ras- (Ras) (Aa and Ab) and JunD-overexpressing Ras-transformed fibroblasts (Ras+JunD) (Ac and Ad). The same phenotype was observed with three independent cell lines. (B) Sections and histological analysis (PECAM-1 immunostaining) of tumors derived from Ras (Ba–Bd) and Ras+JunD (Be–Bh) cells. (C) Vascular density (vessels/mm^2) of total, large-sized (diameter $>$ 30 μm) and small-sized (diameter $<$ 30 μm) blood vessels in Ras- and Ras+JunD-derived tumors. Arrowheads in (B) indicate typical large-sized vessels used for this quantification. Numbers below indicate the percentage of large- and small-sized vessels in the respective populations. Quantification (means $\pm$ SD) resulted from analysis of four independent tumors per cell type and considered at least ten fields for each tumor. Scale bars, 12.5 mm (A) and 200 μm (B).

different AP-1 components (i.e., JunD, c-Jun, JunD+c-Fos, or c-Jun+cFos) with the P-1176 promoter did not modify its activity (data not shown), indicating that JunD controls *VEGF-A* transcription in an indirect manner. This effect might be mediated by the HIF binding site, which has also been removed in the P-888 construct. Accordingly, specific mutation of the HIF binding site in the *VEGF-A* promoter (P-mutHIF) that is known

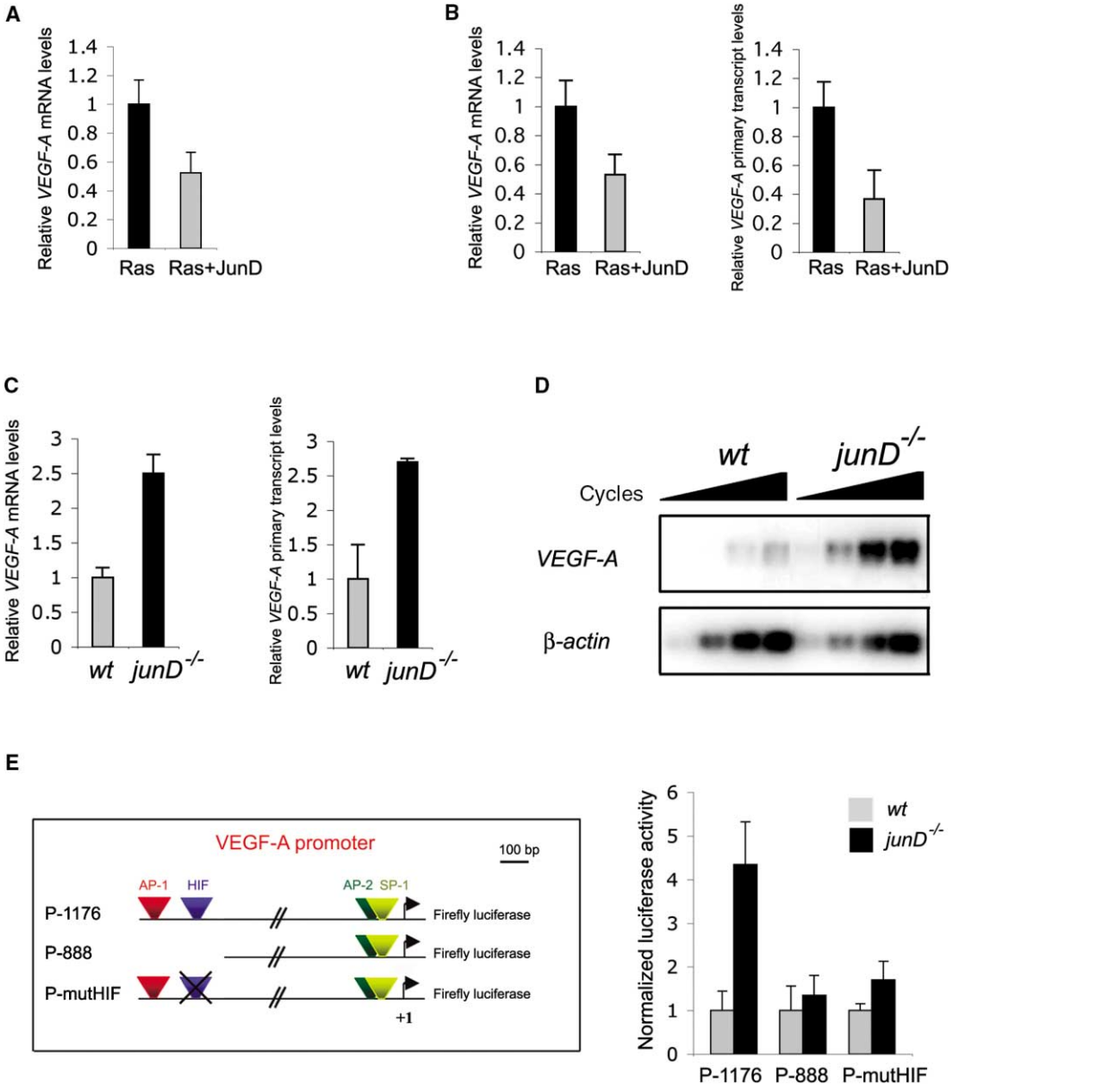

Figure 2. JunD Controls *VEGF-A* Transcription

(A) Relative levels of *VEGF-A* mRNA in Ras and Ras+JunD tumors. β2-microglobulin was used as internal control of amplification. Results are means of four independent tumors per genotype.

(B) Relative levels of *VEGF-A* mRNA (left bar graph) and its primary transcript (right bar graph) in Ras and Ras+JunD independent cell lines. Data are expressed as means ± SD (n = 3 cell lines in triplicate)

(C) Relative levels of *VEGF-A* mRNA (left panel) and its primary transcript (right panel) in wt and *junD*$^{-/-}$ cell lines. Values are means ± SD of experiments reproduced in triplicate for three independent cell lines per genotype.

(D) *VEGF-A* mRNA levels in wt and *junD*$^{-/-}$ embryos (n = 4 embryos per genotype), detected by semiquantitative RT-PCR. β-actin is used as invariant control, and four successive cycles in the linear phase of amplification are shown.

(E) (Left panel) Schematic drawings of the full-length (P-1176) human *VEGF-A* promoter, a deleted version (P-888), and a mutated variant in the HIF binding site (P-mutHIF). The start site of transcription is referred to as +1. (Right panel) Activity of full-length, deleted, and mutated versions of the *VEGF-A* promoter in wt and *junD*$^{-/-}$ fibroblasts. Data are means ± SD (n = 2 cell lines in triplicate).

to abolish HIF-1 DNA binding (Wang and Semenza, 1993) strongly affected the JunD-dependent effect (Figure 2E).

HIF1α and HIF2α Accumulate in *junD*$^{-/-}$ Fibroblasts

To further confirm that the JunD-mediated effect on *VEGF-A* expression was dependent upon HIF, we used the small interfering RNA (siRNA) approach (Figure 3A). HIF-1α siRNA shut down HIF-1α expression, whereas the D-HIF (*Drosophila* HIF) siRNA control had no effect when compared to untreated cells (Figure 3A and see Supplemental Figure S2 at http://www.cell.com/cgi/content/full/118/6/781/DC1). The silencing of HIF-1α was sufficient to suppress the increase of *VEGF-A* tran-

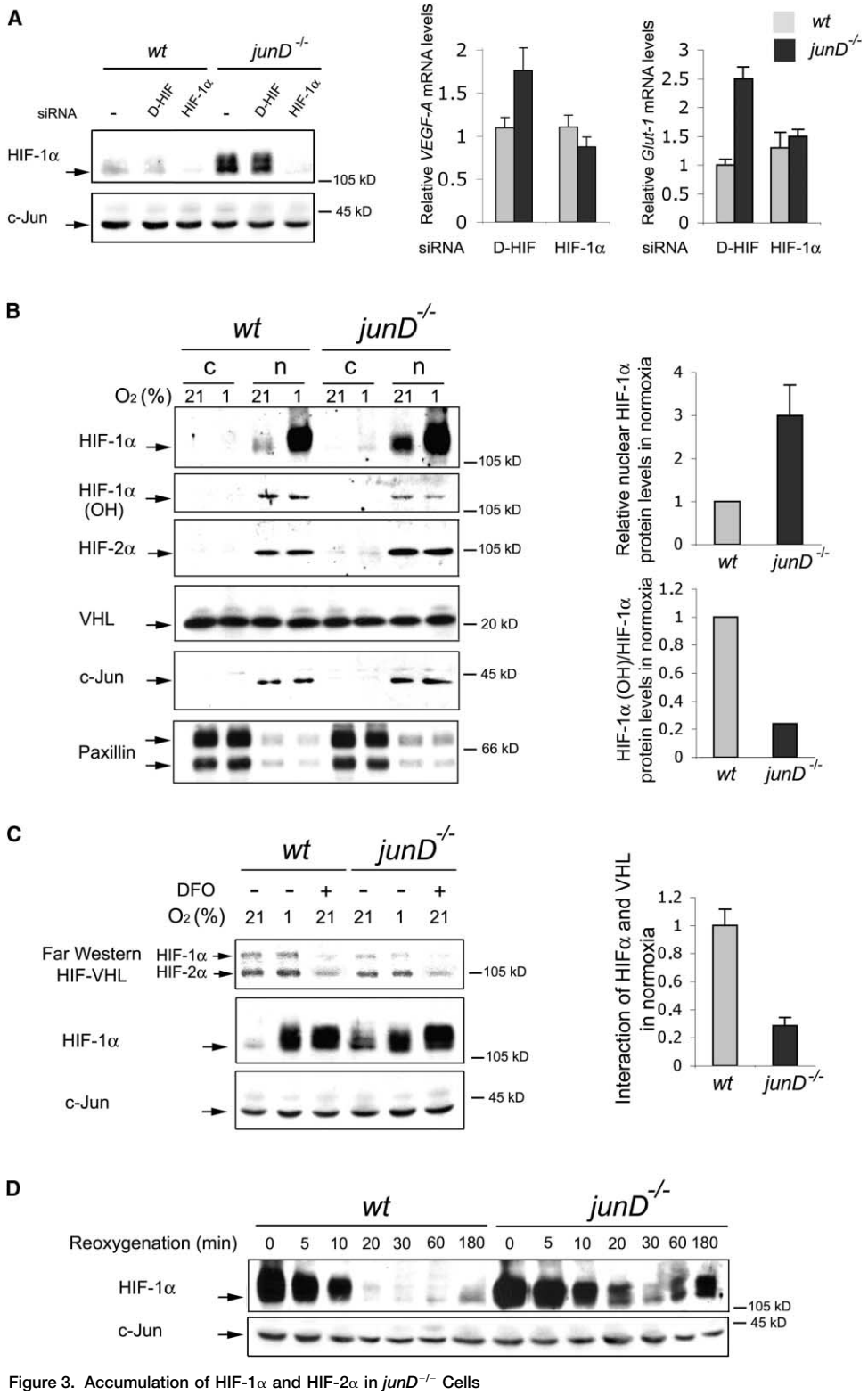

Figure 3. Accumulation of HIF-1α and HIF-2α in *junD*$^{-/-}$ Cells

(A) (Left panel) Western blot showing HIF-1α protein in untransfected (−) wt and *junD*$^{-/-}$ cells or after transfection with the indicated siRNA (upper gel). Endogenous c-Jun protein was used as a loading control (lower gel). Bar graphs, *VEGF-A* and *glut-1* mRNA levels in wt and *junD*$^{-/-}$ clones following HIF-1α silencing.

(B) (Left panel) Representative Western blot of nuclear (n) and cytoplasmic (c) extracts of wt or *junD*$^{-/-}$ cells incubated under normoxic (21% O_2) or hypoxic (1% O_2) conditions. c-Jun and Paxillin proteins were used as internal controls for nuclear and cytoplasmic extracts, respectively. (Right panels) Quantification of the signals for HIF-1α and HIF-1α-OH proteins under normoxia.

(C) Analysis of HIF-1α/VHL interaction using the Far Western method. Whole-cell extracts from normoxic (21%), hypoxic (1%), or DFO-treated cells were blotted with a radiolabeled VHL protein. Interacting HIF-1α and HIF-2α were identified according to their molecular weight. The intensity of the signals under normoxia was plotted in the adjacent bar graph.

(D) HIF-1α half-life was estimated upon reoxygenation of wt and *junD*$^{-/-}$ hypoxic cells (t_0). Time points of the kinetics of reoxygenation are indicated in minutes (min). c-Jun was used as an internal control. Bar graphs are expressed as means ± SD (n = 3 cell lines per genotype in triplicate).

scription in *junD*$^{-/-}$ fibroblasts. Interestingly, this effect was not restricted to *VEGF-A*, since a similar variation was also detected for *glut1*, another well-characterized HIF target gene (Chen et al., 2001).

We next investigated HIF-1α protein content and compartmentalization by preparing nuclear and cytoplasmic extracts from wt and *junD*$^{-/-}$ cell lines (Figure 3B). HIF-1α was detected in the nuclear extracts in all the cell lines used and conditions applied. Quantification of HIF-1α nuclear content under normoxia revealed that the level of HIF-1α was 3-fold higher in *junD*$^{-/-}$ cell lines relative to wt cells. *JunD* deletion also resulted in increased HIF-2α protein levels, although to a lesser extent (Figure 3B). The accumulation of HIF-1α protein in *junD*$^{-/-}$ cells was not due to an increased transcription rate, since *junD* deletion only led to a slight increase of HIF-1α mRNA level (1.3-fold) (see Supplemental Figure S2 on the *Cell* web site). Considering that hydroxylation of HIF-1α targets binding to VHL, we examined the proportion of the hydroxylated form of HIF-1α (HIF-1α-OH) using an antibody that specifically recognizes the hydroxylated protein (Chan et al., 2002). Under normoxia, the ratio of HIF-1α-OH to the total HIF-1α protein level was decreased (4-fold) in all *junD*$^{-/-}$ compared to wt clones (Figure 3B). The reduced level of HIF-1α-OH in *junD*$^{-/-}$ cells implies decreased interaction with VHL, even though its level and cellular localization did not change in *junD*$^{-/-}$ cells (Figure 3B). We followed the interaction of VHL with HIF-1α using the Far Western method (Figure 3C). HIF-1α/VHL interaction was consistently lower in *junD*$^{-/-}$ cell lines compared with controls in normoxic and hypoxic conditions. As expected, HIF-1α/VHL interaction was almost completely lost in wt and *junD*$^{-/-}$ cells treated with desferrioxamine (DFO), an iron chelator that blocks PHD activity. The same observation was made, although to a lesser extent, with HIF-2α. Finally, we confirmed the decreased HIF-1α/VHL interaction in *junD*$^{-/-}$ cells using coimmunoprecipitation on endogenous proteins (data not shown).

A decrease in the interaction with VHL should affect HIF-1α protein stability. We estimated HIF-1α half-life by measuring the time of its degradation upon reoxygenation. The kinetics of HIF-1α degradation were much slower in *junD*$^{-/-}$ cells than in control fibroblasts (Figure 3D). By 180 min post-reoxygenation, HIF-1α protein levels reached basal levels with the initial differences between the two cell lines.

PHD Enzymatic Activity Is Reduced in *junD*$^{-/-}$ Cells

PHDs catalyze HIF-1α hydroxylation, which controls interaction with VHL. No variation in PHD1, PHD2, or PHD3 mRNA levels was observed in *junD*$^{-/-}$ cells (data not shown). PHD2 has been recently demonstrated to control steady-state HIF-1α levels under normoxia (Berra et al., 2003). The PHD2 protein levels remained invariant in *junD*$^{-/-}$ cells compared to wt cells (data not shown). We next investigated endogenous PHD enzymatic activity by performing VHL capture assays (Epstein et al., 2001) using a HIF-1α peptide as substrate for hydroxylation by cell extracts (Figure 4A). Strikingly, the capture of VHL was reproducibly reduced with *junD*$^{-/-}$ extracts compared to wt, indicating that PHD activity was decreased. PHDs are absolutely dependent on O_2, 2-oxoglutarate, and FeII for full activity. Hypoxia and limitation of FeII are thought to allow HIF-1α to escape hydroxylation and hence proteolysis. Physiological concentrations of ascorbate have been shown to promote PHD activity by reduction of FeIII into FeII (Knowles et al., 2003). We found that treatment with ascorbate restored PHD activity in *junD*$^{-/-}$ cells (Figure 4A). Accordingly, ascorbate led to a drastic reduction of HIF-1α protein levels in *junD*$^{-/-}$ cells, suggesting that changes in the FeII/FeIII ratio might be responsible for defective PHD activity in these cells.

We therefore measured the relative amounts of FeII by an usual colorimetric assay and observed that FeII levels were decreased in *junD*$^{-/-}$ fibroblasts relative to wt cells (Figure 4B). Moreover, treatment of *junD*$^{-/-}$ cell lines with ascorbate brought back the FeII amounts to wt levels. A study of FeIII species was performed using electron paramagnetic resonance (EPR) spectroscopy (Figure 4C). EPR is a method of choice for detecting compounds with unpaired electrons and has been extensively used for studying transition metal ions (such as FeIII) in proteins (Ubbink et al., 2002). Positions and shapes of the EPR signals are greatly dependent on the environment of FeIII ion. Moreover, double integration of these signals determined the relative levels of FeIII. The EPR spectrum from wt and *junD*$^{-/-}$ cell lines were similar and exhibited two high-spin FeIII complexes ($g = 6$; $g = 4.23$) and a set of typical low-spin FeIII complexes ($g = 2.24$; $g = 2.01$; and $g = 1.93$) (Supplemental Figure S3 and data not shown) (Figure 4C). Although FeIII proportion remained rather similar at high spin, the proportion of low-spin FeIII complexes was increased in *junD*$^{-/-}$ cells compared to wt. Interestingly, iron-dependent dioxygenases exhibit similar low-spin EPR signals (Rosche et al., 1995). We then tried to determine the proportion of PHD2 in FeIII oxidation state (Figure 4D). To define the PHD2-specific EPR spectrum, we overexpressed it by transient transfection in wt and *junD*$^{-/-}$ fibroblasts (wt+*PHD2; junD*$^{-/-}$+*PHD2*). We observed a clear increase of low-spin signals in PHD2-overexpressing cells, confirming that PHD2 exists at a low-spin state. We displayed, in Figure 4D, the $g = 1.93$ component of these signals. Interestingly, the intensity of the signal corresponding to endogenous or overexpressed PHD2 was always higher in *junD*$^{-/-}$ fibroblasts than in wt cells. These data show that the proportion of PHD2 in FeIII oxidation state was higher in *junD*$^{-/-}$ cells than in wt controls.

ROS Accumulate in *junD*$^{-/-}$ Cells

FeII can be oxidized by H_2O_2 to yield FeIII and hydroxyl radicals by the Fenton reaction: $H_2O_2 + FeII \rightarrow OH^{\cdot} + OH^{-} + FeIII$. The increased proportion of FeIII in *junD*$^{-/-}$ cells suggested that H_2O_2 may accumulate. The amount of oxidants in the three *junD*$^{-/-}$ clones was quantified using a cell-permeant molecule that fluoresces when oxidized by peroxides (CM-H2DCFDA) (Figure 5A). *JunD* deletion strongly enhanced the ROS-specific signal. We confirmed that H_2O_2 accumulated in *junD*$^{-/-}$ cell lines using a quantitative H_2O_2 assay (Figure 5B). Because ascorbate has been proposed to increase FeII levels, we analyzed its effect on H_2O_2 production. Ascorbate

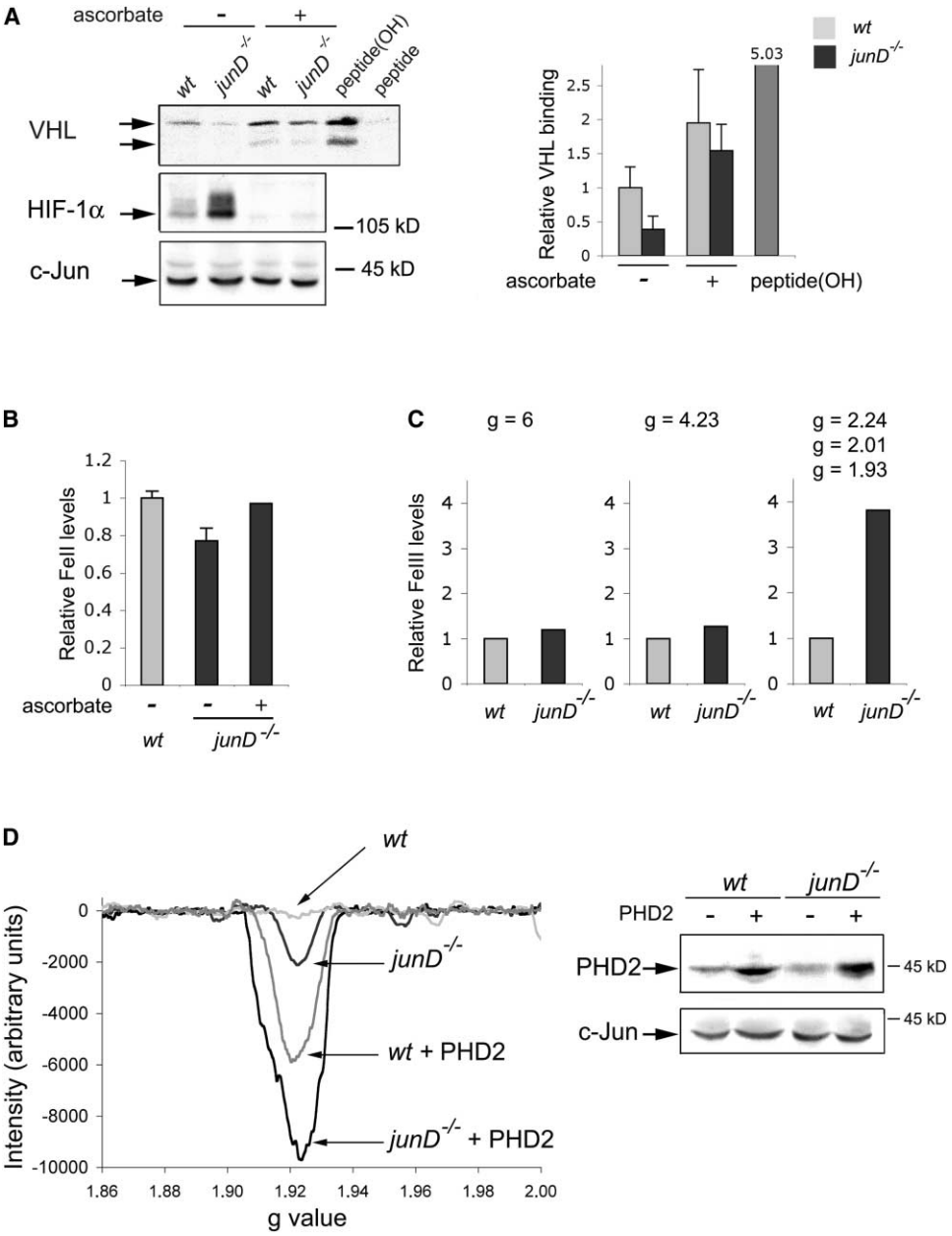

Figure 4. Reduced PHD Activity in *junD*$^{-/-}$ Cells

(A) PHD activity is measured by VHL capture assays using a synthetic peptide (mouse HIF-1α residues 556–574) as substrate (upper gel). Synthetic hydroxylated peptide (peptide OH) is used as positive control. The corresponding amount of HIF-1α is shown in the lower gel with c-Jun as internal control. Right bar graph represents the quantitative data of the VHL capture assays.

(B) Relative levels of FeII in wt or *junD*$^{-/-}$ cell lines determined by a usual colorimetric assay (see Experimental Procedures).

(C) Relative levels of FeIII determined by EPR spectroscopy. EPR signals at g = 6 and g = 4.23 stem from high-spin FeIII-linked complexes in hemoproteins. EPR signals at g = 4.23 correspond to high-spin FeIII in nonheme iron proteins or free iron. Signals at g = 2.24, 2.01, and 1.93 correspond to low-spin FeIII proteins and characterized some dioxygenases. Relative levels of FeIII were determined by double integration of the signals and comparison to a standard solution of $CuCl_2$ (see Experimental Procedures).

(D) (Left panel) EPR signals at g = 1.93 determine the proportion of PHD2 in FeIII oxidation state in wt and *junD*$^{-/-}$ cells overexpressing or not overexpressing PHD2 (wt, *junD*$^{-/-}$, wt+*PHD2; junD*$^{-/-}$+*PHD2)*. (Right panel) Western blot showing PHD2 overexpression in wt and *junD*$^{-/-}$ cells. Bar graphs are expressed as means ± SD (n = 2 cell lines per genotype in triplicate).

treatment abolished H_2O_2 production and decreased HIF-1α protein levels (Figure 5B). Moreover, FeII supplementation ($FeCl_2$) provided FeII ions and restored the PHD enzymatic activity in *junD*$^{-/-}$ cells, thereby reducing HIF-1α protein levels (Figure 5B). Upon FeCl2 supplementation, there were excess FeII ions that also reacted chemically with H_2O_2 through the Fenton reaction, explaining that H_2O_2 levels decreased. Neither ascorbate nor $FeCl_2$ had an effect on the stability of another short-lived protein, c-Jun.

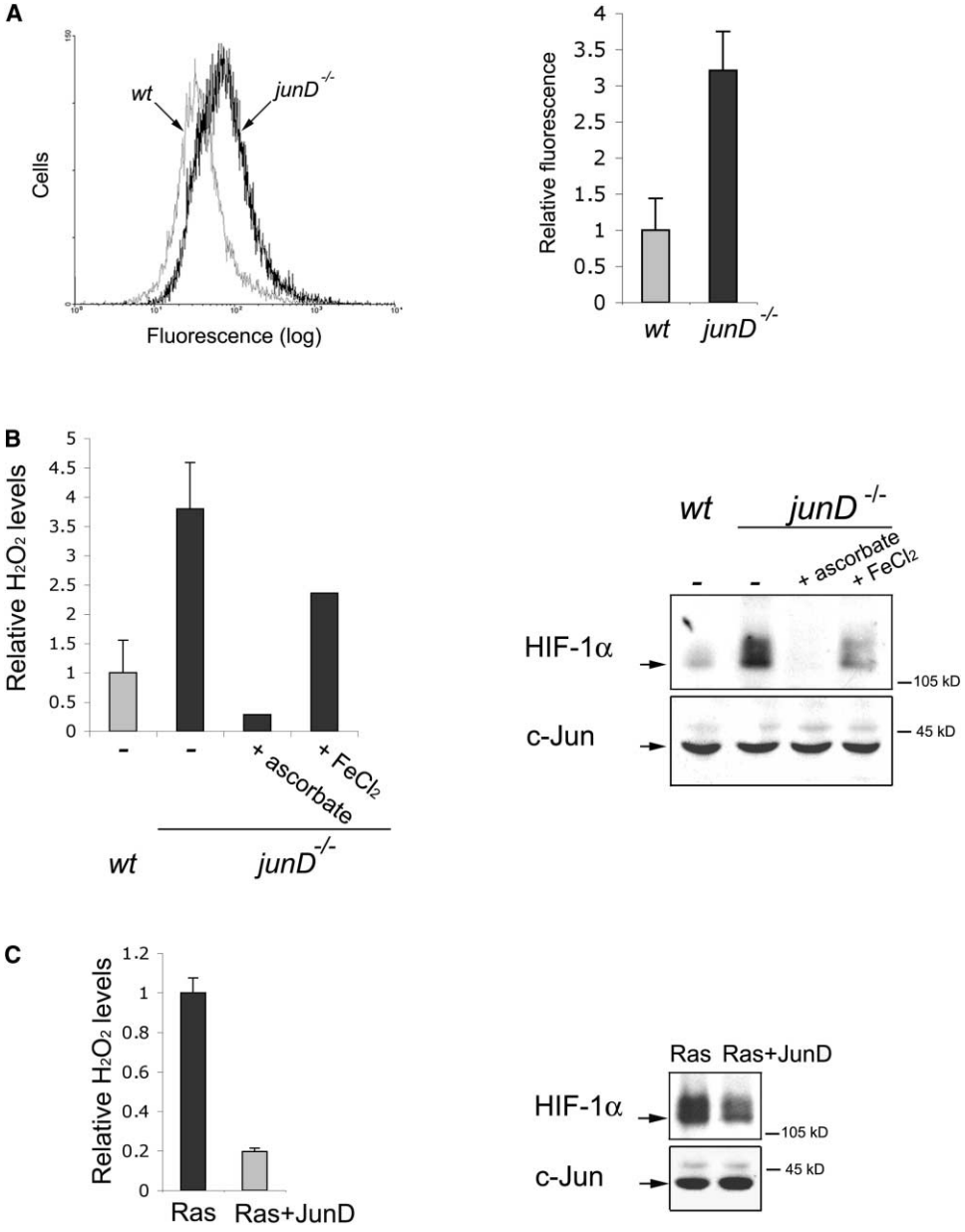

Figure 5. JunD Modulates ROS Production

(A) (Right panel) Relative ROS levels in wt and *junD*$^{-/-}$ clones are measured by using CM-H2DCFDA fluorescence dye. (Left panel) A representative sample for three independent FACS analysis is displayed.

(B) (Left panel) Relative H_2O_2 levels in wt and *junD*$^{-/-}$ cells, in the absence or presence of ascorbate or $FeCl_2$. (Right panel) Western blot showing the effects of ascorbate or $FeCl_2$ on HIF-1α and c-Jun protein levels.

(C) (Left panel) Relative H_2O_2 in Ras and Ras+JunD cell lines. (Right panel) Western blot showing the HIF-1α and c-Jun protein levels. Bar graphs are expressed as means ± SD (n = 3 cell lines per genotype in triplicate).

Ras promotes the production of ROS (Irani et al., 1997) that may influence PHD activity, similarly to *junD* deletion. Since expression of JunD antagonized Ras-induced tumor angiogenesis (Figure 1), we compared H_2O_2 production in Ras and Ras+JunD fibroblasts (Figure 5C). JunD overexpression decreased H_2O_2 and HIF-1α protein levels. This explains the decreased *VEGF-A* transcription rate reported above (Figures 2A and 2B).

Gene Expression Profiling in *junD*-Deficient Cells

To try to unravel how JunD can influence H_2O_2 production, we performed Affymetrix microarray analysis and compared the transcriptome of *junD*$^{-/-}$ versus wt cells. Of the 24,000 tested probe sets, 235 genes or ESTs were downregulated at least 2-fold in *junD*$^{-/-}$ cells, whereas 124 genes or ESTs were upregulated at least 2-fold (D. Gerald, unpublished data). Interestingly, among the genes differentially regulated, we identified a group involved in H_2O_2 metabolism and regulation of oxidative stress (Figure 6). We confirmed the microarray data by QRT-PCR (Figure 7A). Among the downregulated genes were the *microsomal glutathione-S-transferase-1* (*Mgst-1*) (almost undetectable level in *junD*$^{-/-}$ cells) and the *cysteine dioxygenase* (*Cdo1*) (5.5-fold decrease in

Abbreviation	Name of Gene	Level of Expression	Fold Change	Accession Number	Function
Nox4	NADPH Oxidase 4	18.26	3.65	AI043024	Cytoplasmic enzyme involved in H_2O_2 production
Mgst1	Microsomal glutathione S-transferase 1	703.42	-147.39	AW124337	Conjugation of glutathione to electrophiles; reduction of lipids; protection against oxidative damage
RBP4	Retinol binding protein 4, plasma	884.97	-27.87	U63146	Specific carrier for retinol; protection from lipid peroxydation on retinal pigment epithelium
Cp	Ceruloplasmin	1247.29	-10.83	U49430	Copper binding protein; superoxide dismutase activity; release iron from cells in the liver
Rdh10	Retinol dehydrogenase 10	926.56	-5.83	AW047388	Oxidize retinol into retinal; lipid metabolism and peroxydation
Cdo1	Cysteine dioxygenase 1, cytosolic	428.41	-5.58	AI854020	Oxidation of cysteine to cysteine sulfate; acting on single donors with incorporation of oxygen
Ahr	Aryl-hydrocarbon receptor	1132.62	-5.19	M94623	Regulate xenobiotic-metabolizing enzymes such as cytochrome P450
Lactb	Serine beta-lactamase-like protein	145.04	-4.47	AW259606	Serine protease; mitochondrial ribosomal protein
Ptgis	Prostaglandin I2 (prostacyclin) synthase	585.93	-4.14	AB001607	Member of cytochrome P450 family; localized in endoplasmic reticulum membrane
Ldh2	Lactate dehydrogenase 2B	2212.06	-3.66	X51905	Involved in glycolysis; decreased transcription under chronic hypoxia
UBX4	Ubiquitin hydrolase X4	359.13	-3.42	AW122786	Thiol proteases; release of ubiquitin from proteins
Aldh2	Aldehyde dehydrogenase 2	1596.56	-3.11	U07235	Protector against oxidative stress; involved in alcohol metabolism; mitochondrial localization
Cyp1b1	Cytochrome P450, 1b1	2992.39	-2.8	X78445	Oxidative degradation of environmental toxins and mutagens
Aqp1	Aquaporin 1	1656.94	-2.54	L02914	Role in CO2 transport across the human erythrocyte membrane; mitochondrial outer membrane
Dhcr7	7-dehydrocholesterol reductase	397.21	-2.47	AF057368	Cholesterol biosynthesis; oxidoreductase; reticulum endoplasmic localization
Pam	Peptidylglycine alpha-amidating monooxygenase	2387.44	-2.4	U79523	Peptide metabolism; oxidoreductase activity; copper ion binding
Scd1	Stearoyl-coenzyme A desaturase 1	2441.01	-2.05	M21285	Synthesis and regulation of unsaturated fatty acids
G6pd2	Glucose-6-phosphate dehydrogenase 2	1279.81	-2.22	Z84471	Pentose-phosphate pathway; production of NADPH and pentoses
Nsdhl	NAD(P)-dependent steroid dehydrogenase-like	776.93	-2.2	AL021127	Cholesterol metabolism; steroid biosynthesis; oxidoreductase

Figure 6. Gene Expression Profiling in *junD*$^{-/-}$ Cells

Stress-related genes that are differentially expressed in *junD*$^{-/-}$ compared to control cells are listed. Three hybridizations have been performed for each cell type. Levels of expression are the mean of values obtained by the triplicate analysis of wt cells. Fold changes correspond to the differential levels of expression in *junD*$^{-/-}$ fibroblasts versus wt cells. Green, downregulated genes; red, upregulated genes.

junD$^{-/-}$ cells compared to wt cells). We have also detected an upregulation of *NADPH-oxidase 4* (*Nox4*) (3-fold in mutant cells versus wt).

Several genes that protect cells from oxidants were downregulated in *junD*-deficient cells, among them *Mgst-1*, *Cdo1*, *Aldehyde dehydrogenase 2* (*ALDH2*), and *Prostaglandin I2 synthase* (*prostacyclin*). All these genes are involved in protection from toxic compounds. *Mgst1* encodes a major detoxification enzyme that catalyzes the conjugation of glutathione (GSH) to a wide variety of electrophilic compounds and maintains the cytoplasm in a reducing environment (Townsend and Tew, 2003). Addition of reduced GSH to *junD*$^{-/-}$ cells decreased H_2O_2 and HIF-1α amounts to wt levels (Figure 7B). Moreover, cysteine serves as precursor for the biosynthesis of GSH. Since the expression of *Cdo1*, which is involved in cysteine homeostasis, was affected by the *junD* deletion, we have analyzed the effect of adding extra cysteine to the growth media of *junD*$^{-/-}$ cells. Addition of extra cysteine also circumvented accumulation of H_2O_2 and HIF-1α in *junD*$^{-/-}$ cells (Figure 7B). c-Jun protein levels did not vary following addition of these reducing compounds, excluding general effects of these treatments on protein synthesis. Finally, addition of diphenyleneiodonium chloride (DPI), an inhibitor of NADPH-oxidase complexes, in *junD*$^{-/-}$ cells reduced HIF-1α protein levels (data not shown), suggesting that the upregulation of *Nox4* contributed to H_2O_2 increase. Conversely, JunD overexpression in Ras-transformed cells downregulated *Nox4* expression (data not shown), confirming that Nox4 played a key role, at least in part, in *junD*-mediated control of H_2O_2 levels.

Taken together, these results prompted us to propose the following model (Figure 7C). JunD regulates both genes involved in antioxidative defense and H_2O_2 production. *JunD* deletion causes increased intracellular H_2O_2 levels. In its turn, H_2O_2 reduces the proportion of active PHD enzymes by promoting iron oxidation. Increased proportion of PHD in the FeIII-inactivated state limits PHD activity, HIF-1α hydroxylation, and degradation. Subsequently, HIF-1α accumulation enhances *VEGF-A* transcription. Reciprocally, JunD overexpression decreases intracellular H_2O_2 content, alleviates ROS toxic effect, and efficiently counteracts Ras-induced angiogenesis in tumors.

Discussion

In the present study, we have highlighted a new function of JunD, a member of the AP-1 family of transcription factors in oxidative stress and angiogenic switch. Deletion of *junD* increases H_2O_2 levels that inhibit PHD enzymatic activity by limiting FeII levels. Consequently, HIF-1α protein accumulates under normoxic conditions, and the transcription of *VEGF-A* is increased. Reciprocally, by limiting the production of oxidants, overexpression of JunD reduces *VEGF-A* expression and exhibits a potent antiangiogenic effect in tumors derived from Ras-transformed fibroblasts. Finally, by deciphering the mode of action of JunD, we have provided further insights into the mechanism of oxygen-independent regulation of PHD enzymatic activity.

FeII-Dependent Regulation of PHD Enzymes

PHD enzymes require the presence of O_2, 2-oxoglutarate, and FeII at the catalytic site for full activity. Changes in the cellular levels of any of these cofactors can influence hydoxylase activity and its downstream effects on the HIF pathway. In this paper, by dissecting the mode of action of JunD, we provide evidence that enhanced ROS levels promoted oxidation of FeII into FeIII, most probably through the Fenton reaction. Hence, sustained production of ROS reduces the cellular pool of FeII and increases the proportion of PHD in FeIII oxidation state.

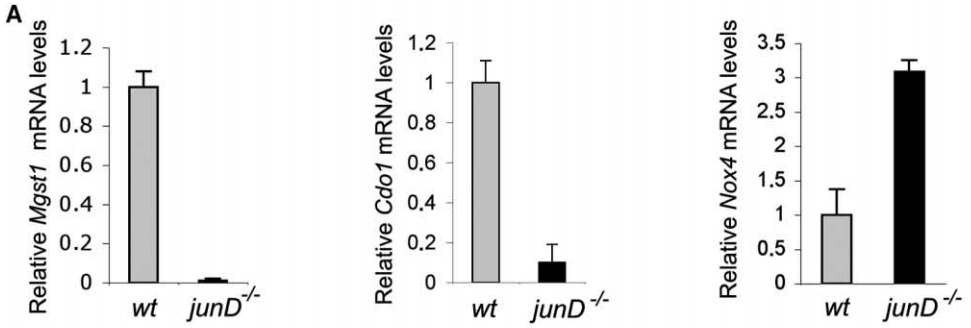

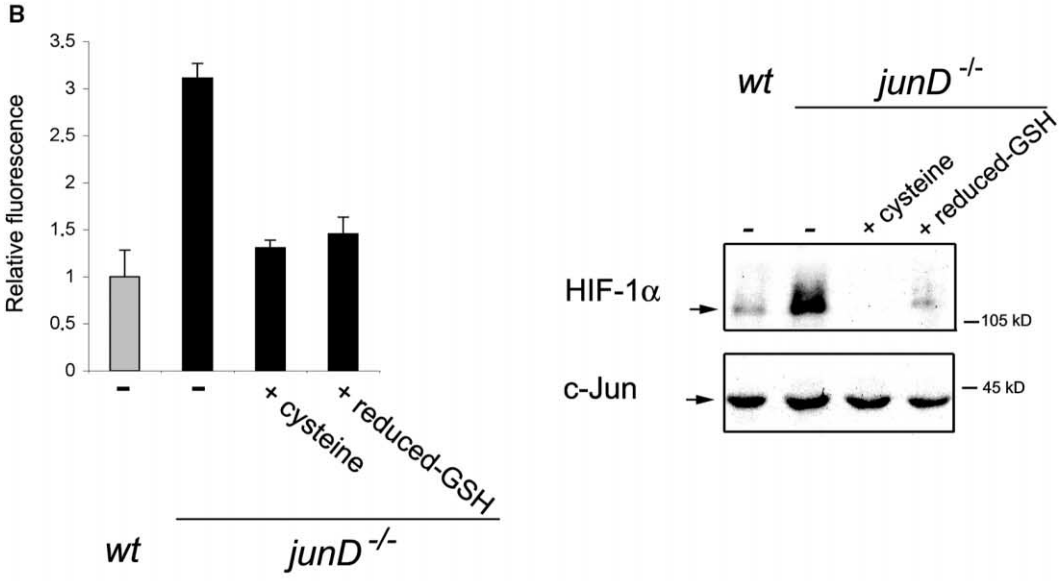

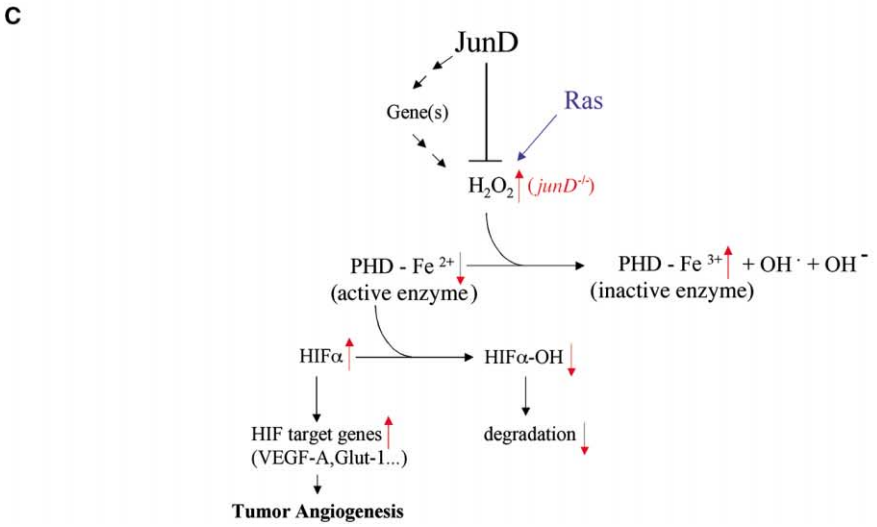

Figure 7. Model for Regulation of ROS and Angiogenesis by JunD

(A) Relative levels of microsomal glutathione S-transferase 1 (*Mgst1*), cysteine dioxygenase (*Cdo1*), and NADPH-oxidase 4 (*Nox4*) in wt and *junD*$^{-/-}$ cells determined by QRT-PCR.

(B) (Left panel) Relative H_2O_2 levels in *junD*$^{-/-}$ cells treated with the indicated reducing agents (reduced glutathione (GSH) and extra cysteine). (Right panel) Corresponding Western blots showing HIF-1α (upper gel) and c-Jun (lower gel) protein levels.

Accordingly, FeII supplementation reduces the steady-state HIF-1α levels in *junD*$^{-/-}$ cells, similarly to the antioxidant compound ascorbate. The effect of ascorbate on FeII availability has been elegantly validated in a recent study (Knowles et al., 2003). Moreover, the iron-dependent regulation of PHD activity has been suggested by studies using cobalt ions (CoII). Cobalt ions are known to inhibit PHD activity. Iron supplementation is sufficient to antagonize HIF-dependent induction of Epo expression by CoII ions. These results strongly suggest that CoII competes with iron and prevents FeII accessibility to the enzymatic site. Our observations validate this model and argue for an iron-mediated regulation of PHD activity under normoxia.

The FeII-dependent regulation of PHD enzymatic activity is most probably shared with other hydroxylases. HIF-1 transcriptional activity is regulated by specific hydroxylation on an asparagine residue that is catalyzed by FIH (factor-inhibiting HIF) (Mahon et al., 2001; Lando et al., 2002). Like PHD, FIH activity is also dependent on O_2, 2-oxoglutarate, and FeII and might be sensitive to limited FeII amounts. *JunD* deletion, through the generation of ROS compounds, could then inhibit FIH enzymatic activity and promote accumulation of transcriptionally active HIF-1α protein.

Role of ROS in the Angiogenic Switch

ROS, such as superoxides and peroxides, act as signal transducers in several systems (for review, see Suzuki et al. [1997]). Previous reports have suggested that H_2O_2 might be required for the induction of HIF-1 activity and the transcription of target genes (Chandel et al., 1998; Agani et al., 2000; Fandrey and Genius, 2000). Production of ROS by cytoplasmic enzymes, including Nox1, a member of the NADPH-oxidase family, has already been shown to induce molecular markers of angiogenesis, such as *VEGF-A* (Arbiser et al., 2002). Moreover, increased ROS generation by Ras-induced *Nox1* is required for oncogenic transformation (Mitsushita et al., 2004). Our data suggest that, in addition to defect in several pathways regulating ROS, NADPH-oxidase complexes may modulate the HIF pathway by triggering ROS production. Moreover, our work uncovers the mechanism of ROS-mediated iron-dependent regulation of PHD enzymatic activity under normoxia.

ROS from any other sources might also promote HIF-1α accumulation. Accordingly, it has been shown that production of ROS from the endoplasmic reticulum is involved in the control of HIF-1α protein levels (Liu et al., 2004). Moreover, mitochondria are major O_2-consuming organelles and are, at least in some circumstances, another major source of ROS. Accumulation of ROS due to mitochondrial dysfunction might also stabilize HIF-1α through iron-mediated inhibition of PHD. If so, HIF-1α might accumulate, under normoxic conditions, in cells deficient for functional mitochondrial respiratory chain. This has been addressed using a genetic approach (Vaux et al., 2001). Analysis of mutant cells lacking mitochondrial DNA (ρ^0 cell lines) revealed that HIF-1α protein levels were higher in some ρ^0 cell lines than in controls under normoxia. We can now speculate that PHDs are in a FeIII-linked inactivated state in these cell lines, although definitive proof requires further investigations. Under hypoxia, lack of O_2 completely shuts down PHD activity and masks iron-dependent regulation of the enzymes. Consistently, HIF-1α stabilization by hypoxia remains normal in ρ^0 cell lines (Srinivas et al., 2001; Vaux et al., 2001).

JunD Protects Cells from Oxidants

Accumulation of ROS, beyond homeostatic thresholds, can cause damage to numerous cellular components, including lipids, proteins, and nucleic acids. Under these conditions, oxidative stress induces an adaptive response and activates antioxidant defense systems that facilitate the breakdown of ROS and assure a redox homeostasis. This cellular adaptative response protects cells from death. One potential outcome associated with chronic oxidative stress in *junD*$^{-/-}$ cells is the previously reported senescence in primary fibroblasts (Weitzman et al., 2000). Moreover, our study demonstrates that JunD-regulated genes are involved in antioxidative response. Indeed, previous studies have shown the role of the evolutionary conserved families of mitogen-activated protein kinases (MAPKs) and AP-1 transcription factors in the response to oxidative stress in distinct species. Pap-1, the yeast homolog of AP-1, participates in the cellular adaptive response to low levels of H_2O_2 (Leppa and Bohmann, 1999; Quinn et al., 2002). Similarly, in fly, JNK signaling pathways coordinate the induction of protective genes that confer tolerance to oxidative stress, alleviate the toxic effects of ROS, and prevent aging (Wang et al., 2003). Among the genes identified in these studies, some (like *Mgst1*) are also differentially regulated in *junD*$^{-/-}$ cells. This indicates a conserved protective function of AP-1 against oxidative stress from yeast to higher vertebrates. A direct role for Jun proteins in the activation of several genes encoding a set of detoxifying defensive proteins has already been reported (Venugopal and Jaiswal, 1998). Antioxidant response elements (ARE), identified in the promoters of genes encoding detoxifying enzymes (such as Mgst), contain active AP-1-like elements. The nuclear transcription factors Nrf2 and Nrf1 have been shown to associate with Jun proteins and positively regulate ARE-mediated expression and coordinated induction of detoxifying enzymes. Taken together, these observations strongly suggest a direct role for JunD in the regulation of antioxidant defense genes that remains to be further investigated.

(C) (Model) PHDs catalyze hydroxylation of proline residues in HIF-1α under normal O_2 conditions. This reaction is required to target HIF-1α for ubiquitination and subsequent proteolysis. PHDs require O_2, FeII, and 2-oxoglutarate for function. A lack of one of these components is sufficient to inhibit PHD enzymatic activity, thereby stabilizing HIF-1α. JunD regulates the expression of genes involved in the control of ROS. Accordingly, *junD* deletion leads to accumulation of H_2O_2. H_2O_2 reduces FeII levels, probably through the Fenton reaction, and inhibits PHD enzymatic activity. HIF-1α is then stabilized, and the expression of HIF target genes, such as *VEGF-A*, increases. Reciprocally, overexpression of JunD is sufficient to reduce the rise of H_2O_2 mediated by Ras transformation and thereby to inhibit tumor angiogenesis. Bar graphs are expressed as means ± SD (n = 2 cell lines per genotype in triplicate).

JunD Displays an Antiangiogenic Effect

Production of ROS and hypoxic response are key players in the occurrence and progression of cancers. The *junD*$^{-/-}$ adult mice do not develop tumors spontaneously (D. Gerald and F. Mechta-Grigoriou, unpublished data), suggesting that the protective effect of JunD may only be uncovered under stress conditions. We revealed a protective effect of JunD in cells transformed by the Ras oncogene, one of the most frequently mutated oncogenes in human cancers. Ras-mediated transformation enhances ROS production, and treatment with antioxidant molecules decreases the proliferation rate of Ras-transformed cell lines (Irani et al., 1997). We previously reported that JunD antagonizes Ras-mediated transformation by modulating cell proliferation (Pfarr et al., 1994). The present study shows that overexpression of JunD decreased ROS production in Ras-transformed cells. Thus, we propose that the inhibitory effect of JunD on the proliferation of Ras-transformed cell lines is mediated in part through the decreased level of ROS. Moreover, Ras oncogene contributes to the growth of solid tumors by a direct effect on cell proliferation and by facilitating tumor angiogenesis. Indeed, transformation by Ras stabilizes HIF-1α and upregulates *VEGF-A* expression as well as other HIF target genes (Bergers and Benjamin, 2003). Furthermore, a recent study has shown that Ras-induced stabilization of HIF-1α is mediated through inhibition of HIF hydroxylation (Chan et al., 2002). Our data confirm these observations and argue that ROS accumulation in Ras-transformed cells triggers PHD inhibition. We show here that JunD has a major effect on this process. Indeed, our findings show that JunD decreased ROS production, restored PHD activity, and subsequently reduced significantly Ras-dependent tumor angiogenesis in vivo. Thus, JunD displays a protective role against Ras-mediated transformation by buffering cells to maintain the redox balance.

In conclusion, our data demonstrate that JunD reduces the activity of an oxygen sensor in the organism by regulating the expression of genes that function in response to oxidative stress and H_2O_2 metabolism. By limiting ROS production and HIF-1α protein stability, JunD decreases the transcription of *VEGF-A*, displays antiangiogenic properties, and is able to counteract Ras-mediated effects. The possibility of modulating JunD activity may open new opportunities to control *VEGF-A* expression in physiological and pathological angiogenesis.

Experimental Procedures

Cell Culture, Transfection, siRNA

Cell culture conditions, Ras, and Ras+JunD cells (three independent clones) have already been described in Pfarr et al. (1994). Three independently derived immortalized cell lines from wt or *junD*$^{-/-}$ embryos were generated using a conventional 3T3 protocol (Todaro and Green, 1963). Experiments were performed at least in triplicate on independent cell lines. For hypoxia, cells were incubated in hypoxic chamber containing 1% O_2 for 3 hr. Treatments of cells were performed for 4 hr with ascorbate (50 μM), $FeCl_2$ (40 μM), DFO (100 μM), reduced GST (2 mM), or extra cysteine (2 mM) (Sigma). Calcium phosphate precipitation method was used for transfection. Luciferase assays were performed using the Dual-Luciferase Reporter Assay System from Promega. Silencing of HIF-1α by siRNA was performed as previously described (Berra et al., 2003). The siRNA sequences targeting mouse HIF-1α and D-HIF correspond to the coding regions 1729–1747 and 2557–2575, relative to the start codon. Mutation of the human *VEGF-A* promoter in the HIF binding site proceeded using the QuickChange Site-Directed Mutagenesis Kit (Stratagene) (5′**CGT**G3′ → 5′**AAA**G3′).

Analysis of Gene Expression

Total RNAs were isolated using RNeasy Kit (Qiagen) and treated by DNaseI (DNase I $RNase_{free}$, Roche) followed by a phenol/chloroform extraction for DNase inactivation. cDNA were prepared from 1 μg total RNA using random hexaprimers as templates and SuperScript II (Invitrogen). Absence of DNA contamination was verified by performing amplification without RTase. Quantitative real-time RT-PCR was carried out on an AbiPrism 7000 system using SYBR Green. The four isoforms that correspond to the spliced variants of *VEGF-A* mRNA were amplified (Tischer et al., 1991). Intron 4 was amplified to detect *VEGF-A* primary transcript. The primer sequences are available upon request. For the Affymetrix GeneChip probe array, three RNA samples were pooled according to their genotype. Pooled RNA were used to synthetize cRNA and hybridized to Affymetrix Murine Genome U74v2 A and B GeneChips. We performed three successive hybridizations to limit experimental variations. Detected probe sets were selected according to the "presence calls" of Microarray Suite Software MAS 5.0 (Affymetrix). Fold change of expression between wt and *junD*$^{-/-}$ cells were established using the dChip 1.3 software (Li and Wong, 2001). Only significantly changed probe sets ($p < 0.05$) were taken into account.

Cell Extracts and Immunoblot Analysis

Cell extracts and Western blotting were performed as in Mechta et al. (1997). Antibodies recognizing mouse c-Jun protein (Lallemand et al., 1997), HIF-1α (Richard et al., 2000), hydroxylated HIF-1α (Chan et al., 2002), pVHL (Pharmingen-Ig32), Paxillin (Transduction Laboratories-P13520), and HIF-2α (Abcam-ab199) were used. Blots were incubated with horseradish peroxidase-conjugated secondary antibody followed by detection with enhanced chemoluminescence (Amersham) and exposed to autoradiography films. Quantifications were performed using ImageQuant software (Molecular Dynamics).

Far Western

Far Western analysis was previously described in Guichet et al. (1997). In brief, the full-length mouse VHL protein was in vitro translated using a TNT Transcription/Translation Kit (Promega) to produce VHL ^{35}S probe. Unincorporated nucleotides were removed in a Bio-Rad G25 resin column. Blots were incubated with 100 μl labeled VHL protein in 2 ml buffer (0.1 M NaCl, 20 mM Tris (pH 7.6), 1 mM EDTA, 1 mM DTT, 10% glycerol, and 1% milk powder) overnight at 4°C. Membranes were washed in the above buffer at 4°C, dried, autoradiographed, and quantified.

In Vitro PHD Activity

Assay for interaction between VHL and synthetic biotinylated HIF-1α peptides was described in Epstein et al. (2001). Peptides were synthesized by Millegen. Streptavidin-associated peptides (5 μg) were preincubated with cell lysates (150 μg) 1 hr at 28°C, washed, and mixed with in vitro ^{35}S-labeled VHL. Bound VHL was analyzed by SDS-PAGE, autoradiographed, and quantified.

Measurement of Intracellular ROS and H_2O_2

Intracellular ROS generation was assessed using 5-(and 6-)chloromethyl-2′,7′-dichlorodihydrofluorescein diacetate (CM-H_2DCFDA) (Molecular Probes). Cells were incubated for 1 hr with 5 μM CM-H_2DCFDA, harvested and resuspended at 10^6 cells/ml in PBS supplemented with 7% FCS, and subjected to FACscan analysis. A minimum of 30,000 cells was sampled per condition. The concentration of cellular H_2O_2 was determined with a quantitative H_2O_2 assay kit, according to the protocol provided by the manufacturer (Sigma-PD1). Briefly, cells were lysed and incubated at room temperature with a xylenol orange solution; absorbance was then detected at 560 nm using a spectrophotometer (Bio-Tek).

Iron Measurements

FeII levels were measured using a standard analytical procedure (Feger et al., 2001). In brief, 3×10^6 cells were lysed in 1 N HCl and incubated with a chromogenic chelator (Na-bathophenanthrolinsulfonat) (100 μM). Absorbance was then detected at 550 nm. EPR spectroscopy has been performed on a Bruker Elexsys 500 spectrometer with an SHQ001 cavity fitted with an ESR900 cooling system. The microwave source operated at 9.34 GHz. The spectra have been recorded at 12 kelvin (K) using 15×10^6 cells. Cells were harvested in PBS, centrifuged into 3 mm quartz tubes at 1500 rpm, and frozen in liquid nitrogen. In general, the spectra were obtained as four added scans from 1 to 500 mT using time constant 0.01024 s, a modulation amplitude of 1.5 mT, and a modulation frequency of 100 kHz. Quantification of the EPR signals was performed by double integration of the spectra recorded under nonsaturating conditions and by comparison with a standard (30 μM $CuCl_2$ and 300 μM EDTA) (Cammack and Cooper, 1993).

Tumor Vascularization Assays

Tumors were generated as described in Pfarr et al. (1994) using 5×10^5 cells per injection. Tumors were dissected out 15–20 days after injection. For sectioning, parts of tumors were embedded in gelatine 15% sucrose 7.5% containing matrix, and 20 μm sections were obtained by using a cryostat. Sections were immunostained using a specific anti-PECAM-1 antibody (MEC 13.3 from Pharmingen).

Acknowledgments

We thank O. Bluteau and D. Lallemand for fruitful discussions and critical comments on this work. We are grateful to D. Philpott and J.B. Weitzman for critical reading of the manuscript. We acknowledge the expert contribution of the Affymetrix platform at the Curie Institute in Paris and the help of M. Pontoglio and S. Garbay in microarray analysis. We also thank G. Pages for the kind gift of *VEGF-A* promoter constructs and Jean-Luc Boucher for help in EPR sample preparation. This work was supported by grants from the Ministere de l'Education Nationale, de la Recherche et de la Technologie, the European Community Biomed and Training Mobility programs, the Ligue Nationale Contre le Cancer Ile de France, and the Association pour la Recherche sur le Cancer.

Received: March 15, 2004
Revised: July 23, 2004
Accepted: July 27, 2004
Published: September 16, 2004

References

Agani, F.H., Pichiule, P., Chavez, J.C., and LaManna, J.C. (2000). The role of mitochondria in the regulation of hypoxia-inducible factor 1 expression during hypoxia. J. Biol. Chem. *275*, 35863–35867.

Arbiser, J.L., Petros, J., Klafter, R., Govindajaran, B., McLaughlin, E.R., Brown, L.F., Cohen, C., Moses, M., Kilroy, S., Arnold, R.S., and Lambeth, J.D. (2002). Reactive oxygen generated by Nox1 triggers the angiogenic switch. Proc. Natl. Acad. Sci. USA *99*, 715–720.

Barbacid, M. (1987). ras genes. Annu. Rev. Biochem. *56*, 779–827.

Benjamin, L.E., and Keshet, E. (1997). Conditional switching of vascular endothelial growth factor (VEGF) expression in tumors: induction of endothelial cell shedding and regression of hemangioblastoma-like vessels by VEGF withdrawal. Proc. Natl. Acad. Sci. USA *94*, 8761–8766.

Bergers, G., and Benjamin, L.E. (2003). Tumorigenesis and the angiogenic switch. Nat. Rev. Cancer *3*, 401–410.

Berra, E., Benizri, E., Ginouves, A., Volmat, V., Roux, D., and Pouyssegur, J. (2003). HIF prolyl-hydroxylase 2 is the key oxygen sensor setting low steady-state levels of HIF-1alpha in normoxia. EMBO J. *22*, 4082–4090.

Bos, J.L. (1989). ras oncogenes in human cancer: a review. Cancer Res. *49*, 4682–4689.

Bruick, R.K., and McKnight, S.L. (2001). A conserved family of prolyl-4-hydroxylases that modify HIF. Science *294*, 1337–1340.

Cammack, R., and Cooper, C.E. (1993). Electron paramagnetic spectroscopy of iron complexes and iron-containing proteins. Methods Enzymol. *227*, 353–384.

Chan, D.A., Sutphin, P.D., Denko, N.C., and Giaccia, A.J. (2002). Role of prolyl hydroxylation in oncogenically stabilized hypoxia-inducible factor-1alpha. J. Biol. Chem. *277*, 40112–40117.

Chandel, N.S., Maltepe, E., Goldwasser, E., Mathieu, C.E., Simon, M.C., and Schumacker, P.T. (1998). Mitochondrial reactive oxygen species trigger hypoxia-induced transcription. Proc. Natl. Acad. Sci. USA *95*, 11715–11720.

Chen, C., Pore, N., Behrooz, A., Ismail-Beigi, F., and Maity, A. (2001). Regulation of glut1 mRNA by hypoxia-inducible factor-1. Interaction between H-ras and hypoxia. J. Biol. Chem. *276*, 9519–9525.

Epstein, A.C., Gleadle, J.M., McNeill, L.A., Hewitson, K.S., O'Rourke, J., Mole, D.R., Mukherji, M., Metzen, E., Wilson, M.I., Dhanda, A., et al. (2001). *C. elegans* EGL-9 and mammalian homologs define a family of dioxygenases that regulate HIF by prolyl hydroxylation. Cell *107*, 43–54.

Fandrey, J., and Genius, J. (2000). Reactive oxygen species as regulators of oxygen dependent gene expression. Adv. Exp. Med. Biol. *475*, 153–159.

Feger, F., Ferry-Dumazet, H., Mamani Matsuda, M., Bordenave, J., Dupouy, M., Nussler, A.K., Arock, M., Devevey, L., Nafziger, J., Guillosson, J.J., et al. (2001). Role of iron in tumor cell protection from the pro-apoptotic effect of nitric oxide. Cancer Res. *61*, 5289–5294.

Ferrara, N., Gerber, H.P., and LeCouter, J. (2003). The biology of VEGF and its receptors. Nat. Med. *9*, 669–676.

Folkman, J. (1990). What is the evidence that tumors are angiogenesis dependent? J. Natl. Cancer Inst. *82*, 4–6.

Giaccia, A., Siim, B.G., and Johnson, R.S. (2003). HIF-1 as a target for drug development. Nat. Rev. Drug Discov. *2*, 803–811.

Guichet, A., Copeland, J.W., Erdelyi, M., Hlousek, D., Zavorszky, P., Ho, J., Brown, S., Percival-Smith, A., Krause, H.M., and Ephrussi, A. (1997). The nuclear receptor homologue Ftz-F1 and the homeodomain protein Ftz are mutually dependent cofactors. Nature *385*, 548–552.

Ikeda, E., Achen, M.G., Breier, G., and Risau, W. (1995). Hypoxia-induced transcriptional activation and increased mRNA stability of vascular endothelial growth factor in C6 glioma cells. J. Biol. Chem. *270*, 19761–19766.

Irani, K., Xia, Y., Zweier, J.L., Sollott, S.J., Der, C.J., Fearon, E.R., Sundaresan, M., Finkel, T., and Goldschmidt-Clermont, P.J. (1997). Mitogenic signaling mediated by oxidants in Ras-transformed fibroblasts. Science *275*, 1649–1652.

Ivan, M., Kondo, K., Yang, H., Kim, W., Valiando, J., Ohh, M., Salic, A., Asara, J.M., Lane, W.S., and Kaelin, W.G., Jr. (2001). HIFα targeted for VHL-mediated destruction by proline hydroxylation: implications for O2 sensing. Science *292*, 464–468.

Jaakkola, P., Mole, R.D., Tian, Y.M., Wilson, M.I., Gielbert, J., Gaskell, S.J., Von Kriegsheim, A., Hebenstreit, H.F., Mukherji, M., Schofiels, C.J., et al. (2001). Targeting of HIF-α to the von Hippel-Lindau ubiquitylation complex by O2-regulated prolyl hydroxylation. Science *292*, 468–472.

Kim, W., and Kaelin, W.G., Jr. (2003). The von Hippel-Lindau tumor suppressor protein: new insights into oxygen sensing and cancer. Curr. Opin. Genet. Dev. *13*, 55–60.

Knowles, H.J., Raval, R.R., Harris, A.L., and Ratcliffe, P.J. (2003). Effect of ascorbate on the activity of hypoxia-inducible factor in cancer cells. Cancer Res. *63*, 1764–1768.

Kovary, K., and Bravo, R. (1991). The jun and fos protein families are both required for cell cycle progression in fibroblasts. Mol. Cell. Biol. *11*, 4466–4472.

Lallemand, D., Spyrou, G., Yaniv, M., and Pfarr, C.M. (1997). Variations in Jun and Fos protein expression and AP1 activity in cycling, resting, and stimulated fibroblasts. Oncogene *14*, 819–830.

Lando, D., Peet, D.J., Whelan, D.A., Gorman, J.J., and Whitelaw, M.L. (2002). Asparagine hydroxylation of the HIF transactivation domain a hypoxic switch. Science *295*, 858–861.

Leppa, S., and Bohmann, D. (1999). Diverse functions of JNK signal-

ing and c-Jun in stress response and apoptosis. Oncogene *18*, 6158–6162.

Li, C., and Wong, W.H. (2001). Model-based analysis of oligonucleotide arrays: expression index computation and outlier detection. Proc. Natl. Acad. Sci. USA *98*, 31–36.

Liu, Q., Berchner-Pannschmidt, U., Moller, U., Brecht, M., Wotzlaw, C., Acker, H., Jungermann, K., and Kietzmann, T. (2004). A Fenton reaction at the endoplasmic reticulum is involved in the redox control of hypoxia-inducible gene expression. Proc. Natl. Acad. Sci. USA *101*, 4302–4307.

Mahon, P.C., Hirota, K., and Semenza, G.L. (2001). FIH-1: a novel protein that interacts with HIF-1α and VHL to mediate repression of HIF-1 transcriptional activity. Genes Dev. *15*, 2675–2686.

Mechta, F., Lallemand, D., Pfarr, C.M., and Yaniv, M. (1997). Transformation by ras modifies AP1 composition and activity. Oncogene *14*, 837–847.

Mechta-Grigoriou, F., Gerald, D., and Yaniv, M. (2001). The mammalian Jun proteins: redundancy and specificity. Oncogene *20*, 2378–2389.

Mitsushita, J., Lambeth, J.D., and Kamata, T. (2004). The superoxide-generating oxidase Nox1 is functionally required for Ras oncogene transformation. Cancer Res. *64*, 3580–3585.

Peeper, D., Upton, T., Ladha, M., Neuman, E., Zalvide, J., Bernards, R., DeCaprio, J., and Ewen, M. (1997). Ras signalling linked to the cell-cycle machinery by the retinoblastoma protein. Nature *386*, 177–181.

Pfarr, C.M., Mechta, F., Spyrou, G., Lallemand, D., Carillo, S., and Yaniv, M. (1994). Mouse JunD negatively regulates fibroblast growth and antagonizes transformation by ras. Cell *76*, 747–760.

Pugh, C.W., and Ratcliffe, P.J. (2003a). Regulation of angiogenesis by hypoxia: role of the HIF system. Nat. Med. *9*, 677–684.

Pugh, C.W., and Ratcliffe, P.J. (2003b). The von Hippel-Lindau tumor suppressor, hypoxia-inducible factor-1 (HIF-1) degradation, and cancer pathogenesis. Semin. Cancer Biol. *13*, 83–89.

Quinn, J., Findlay, V.J., Dawson, K., Millar, J.B., Jones, N., Morgan, B.A., and Toone, W.M. (2002). Distinct regulatory proteins control the graded transcriptional response to increasing H_2O_2 levels in fission yeast Schizosaccharomyces pombe. Mol. Biol. Cell *13*, 805–816.

Richard, D.E., Berra, E., and Pouyssegur, J. (2000). Nonhypoxic pathway mediates the induction of hypoxia-inducible factor 1α in vascular smooth muscle cells. J. Biol. Chem. *275*, 26765–26771.

Rosche, B., Fetzner, S., Lingens, F., Nitschke, W., and Riedel, A. (1995). The 2Fe2S centres of the 2-oxo-1,2-dihydroquinoline 8-monooxygenase from Pseudomonas putida 86 studied by EPR spectroscopy. Biochim. Biophys. Acta *1252*, 177–179.

Semenza, G.L. (1999). Regulation of mammalian O2 homeostasis by hypoxia-inducible factor 1. Annu. Rev. Cell Dev. Biol. *15*, 551–578.

Shaulian, E., and Karin, M. (2002). AP-1 as a regulator of cell life and death. Nat. Cell Biol. *4*, E131–E136.

Srinivas, V., Leshchinsky, I., Sang, N., King, M.P., Minchenko, A., and Caro, J. (2001). Oxygen sensing and HIF-1 activation does not require an active mitochondrial respiratory chain electron-transfer pathway. J. Biol. Chem. *276*, 21995–21998.

Suzuki, Y.J., Forman, H.J., and Sevanian, A. (1997). Oxidants as stimulators of signal transduction. Free Radic. Biol. Med. *22*, 269–285.

Tischer, E., Mitchell, R., Hartman, T., Silva, M., Gospodarowicz, D., Fiddes, J.C., and Abraham, J.A. (1991). The human gene for vascular endothelial growth factor. Multiple protein forms are encoded through alternative exon splicing. J. Biol. Chem. *266*, 11947–11954.

Todaro, G.J., and Green, H. (1963). Quantitative studies of the growth of mouse embryo cells in culture and their development into established lines. J. Cell Biol. *17*, 299–313.

Townsend, D.M., and Tew, K.D. (2003). The role of glutathione-S-transferase in anti-cancer drug resistance. Oncogene *22*, 7369–7375.

Ubbink, M., Worrall, J.A., Canters, G.W., Groenen, E.J., and Huber, M. (2002). Paramagnetic resonance of biological metal centers. Annu. Rev. Biophys. Biomol. Struct. *31*, 393–422.

Vaux, E.C., Metzen, E., Yeates, K.M., and Ratcliffe, P.J. (2001). Regulation of hypoxia-inducible factor is preserved in the absence of a functioning mitochondrial respiratory chain. Blood *98*, 296–302.

Venugopal, R., and Jaiswal, A.K. (1998). Nrf2 and Nrf1 in association with Jun proteins regulate antioxidant response element-mediated expression and coordinated induction of genes encoding detoxifying enzymes. Oncogene *17*, 3145–3156.

Wagner, E.F. (2001). AP-1—Introductory remarks. Oncogene *20*, 2334–2335.

Wang, G.L., and Semenza, G.L. (1993). General involvement of hypoxia-inducible factor 1 in transcriptional response to hypoxia. Proc. Natl. Acad. Sci. USA *90*, 4304–4308.

Wang, M.C., Bohmann, D., and Jasper, H. (2003). JNK signaling confers tolerance to oxidative stress and extends lifespan in *Drosophila*. Dev. Cell *5*, 811–816.

Weitzman, J.B., Fiette, L., Matsuo, K., and Yaniv, M. (2000). JunD protects cells from p53-dependent senescence and apoptosis. Mol. Cell *6*, 1109–1119.

Wenger, R.H. (2002). Cellular adaptation to hypoxia: O2-sensing protein hydroxylases, hypoxia-inducible transcription factors, and O2-regulated gene expression. FASEB J. *16*, 1151–1162.

Wisdom, R., Johnson, R.S., and Moore, C. (1999). c-Jun regulates cell cycle progression and apoptosis by distinct mechanisms. EMBO J. *18*, 188–197.